Preparation and thermoelectric properties of semiconducting Zn_4Sb_3

T. Caillat*, J. -P. Fleurial, and A. Borshchevsky

Jet Propulsion Laboratory/California Institute of Technology
4800 Oak Grove Drive
Pasadena, CA 91109 USA
*e-mail: thierry.caillat@jpl.nasa.gov

ABSTRACT

Hot-pressed samples of the semiconducting compound β-Zn_4Sb_3 were prepared and characterized by x-ray and microprobe analysis. Some physical properties of β-Zn_4Sb_3 were determined and its thermoelectric properties measured between room temperature and 650K. Exceptionally low thermal conductivity values were measured in the 300 to 650K temperature range and the room temperature lattice thermal conductivity was estimated at 6.5 W cm^{-1} K^{-1}. High thermoelectric figures of merit ZTs were obtained between 450 and 670K and a maximum of about 1.3 was obtained at a temperature of 670K, the highest known at this temperature. The stability of the compound was investigated by several techniques, including thermogravimetric studies. The results showed that the samples were stable under argon atmosphere and static vacuum up to about 670K and up to 520K in dynamic vacuum. The high thermoelectric performance of β-Zn_4Sb_3 in the 300 to 670K temperature range fills the existing gap in the ZT spectrum of p-type state-of-the-art thermoelectric materials between Bi_2Te_3-based alloys and PbTe-based alloys. This material, relatively inexpensive, could be used in more efficient thermoelectric generators for waste heat recovery and automobile industry applications, for example.

Keywords: A. semiconductors, D. thermal conductivity D. transport properties.

1. INTRODUCTION

A growth of commercial applications of thermoelectric devices depends primarily on increasing the figure of merit Z of the materials used in the devices. The figure of merit is defined as $Z = \alpha^2\sigma/\lambda$ where α is the Seebeck coefficient, σ the electrical conductivity, and λ the thermal conductivity. Established thermoelectric materials used in power generation can be divided into three categories depending on their temperature range of application. Bismuth telluride and its alloys work around room temperature and have a maximum operating temperature of about 500K. In the intermediate temperature range (600-900K), PbTe-based alloys and TAGS (Te-Ag-Ge-Sb) are the most efficient materials. At the highest temperatures (1000-1300K), Si-Ge alloys are used in power generation devices mainly for space applications. Despite its low efficiency, $FeSi_2$ has also been used in power generation thermoelectric devices because it is inexpensive which is a critical criteria for some applications. Thermoelectric devices are reliable, operate unattended in hostile environments and are also environmentally friendly but new more efficient materials are needed to expand their range of applications.

Based on literature data and theoretical considerations, several new potentially high performance thermoelectric materials were identified over the past few years at the Jet Propulsion Laboratory (JPL). Among them, materials with the skutterudite structure appear very promising. A number of recent papers have appeared describing the thermoelectric properties of the skutterudites [1-10]. More recently, high ZT values have been obtained for several filled skutterudite compositions [11-12]. In addition to skutterudites, JPL determined that several other compounds had a good potential for thermoelectric applications. As part of the broad search for more efficient thermoelectric materials, we have prepared and investigated the properties of the semiconducting compound Zn_4Sb_3. Three compounds have been clearly identified in the Zn-Sb system: ZnSb decomposing peritectically at 819K, Zn_4Sb_3 melting congruently at 836K, and Zn_3Sb_2 melting congruently at 839K [13,14]. For Zn_4Sb_3, three modifications are known: α-, β-, γ-Zn_4Sb_3 which are stable below 263K, between 263 and 765K, and above 765K, respectively. The phase diagram has been re-investigated by Mayer et al.[13]. β-Zn_4Sb_3 has a hexagonal rhombohedric crystal structure, space group R3C with a = 12.231 Å and c = 12.428 Å [13,15]. Low thermal conductivity values can be expected because of its relatively complex structure [13]. To our knowledge, the only thermal conductivity data available in the literature was published by Spitzer [16] who reported a room temperature lattice thermal conductivity value of 6.5 $mWcm^{-1}K^{-1}$ on a polycrystalline sample of unknown density. A few investigations of the electrical and thermoelectric properties of β-Zn_4Sb_3 were performed [15,17,18] but the results were somewhat inconsistent. Some attempts were also made to dope the compound with various dopants [19]. The optical properties were investigated and an optical band gap of about 1.2 eV was measured [15], in agreement with one estimation made from high temperature electrical measurements [17]. Some questions about the stability of this compound were also raised [15]. We examined the thermoelectric and some other properties of polycrystalline samples of β-Zn_4Sb_3 and investigated its temperature stability to assess its usefulness for thermoelectric applications.

2. EXPERIMENTAL

Although crystals of β-Zn_4Sb_3 were grown [15,18], it has been difficult to obtain large crack-free samples. This is likely due to the phase transformation occurring upon cooling at 765K. The γ-Zn_4Sb_3 and β-Zn_4Sb_3 phases might have different coefficient of expansion, resulting in stresses during cooling and causing the crack formation. Single phase, polycrystalline samples of β-Zn_4Sb_3 were prepared. First, zinc (99.9999% pure) and antimony shots (99.999% pure) in stoichiometric ratio were melted in sealed quartz ampoules. The melts were held at 1023K for about 2 hours for homogenization and quenched in water. Resulting ingots were ground in an agate mortar and analyzed by x-ray diffractometry (XRD) which showed that the powders were single phase after quenching. The powders were sieved and only grains with a size of 125 μm or less were retained for further processing. The pre-synthesized powders were then hot-pressed into cylindrical samples. The hot-pressing was conducted in graphite dies. The samples (about 12 mm in diameter and about 2 cm long) were crack-free and of good mechanical strength. Microprobe analysis showed that the samples were single phase after hot-pressing. A total of 20 samples were fabricated.

The density of the samples was measured by the immersion technique using toluene as the liquid. The density of the hot-pressed samples was typically between 96 and 98% of the theoretical density. Microprobe analysis of selected samples was performed on a JEOL JXA-733 superprobe. XRD analyses were performed on a Siemens D-500 diffractometer using Cu-K_α radiation with silicon as a standard. The thermal expansion coefficient was measured using a standard dilatometer. The shear and longitudinal sound velocity were measured at room temperature on a few samples about 12 mm long using a frequency of 5 Mhz. Thermogravimetric analysis (TGA) were conducted on a Dupont-2000 thermogravimetric measurements apparatus, using argon as the purge gas.

Samples about 1 mm thick and 12 mm in diameter were cut from the hot-pressed specimens (perpendicular to the hot-pressing direction) for transport property measurements. Resistivity and Hall effect measurements were conducted between room temperature and about 673K in static or dynamic vacuum. The electrical resistivity (ρ) was measured using the van der Pauw technique with a current of 100 mA using a special high temperature apparatus [20]. The Hall coefficient (R_H) was measured in the same apparatus with a constant magnetic field value of 10500 Gauss. Assuming a scattering factor of 1 in a single carrier scheme, the carrier density was calculated from the Hall coefficient by $p=1/R_H e$ where p is the density of holes and e is the electron charge. The Hall mobility (μ_H) was calculated from the Hall coefficient and the resistivity values by $\mu_H = R_H/\rho$. The error was estimated at ± 0.5% and ±

2% for the resistivity and Hall coefficient measurements, respectively. The Seebeck coefficient (α) of the samples was measured on the same samples used for resistivity and Hall coefficient measurements using a high temperature light pulse technique [21]. The error of measurements of the Seebeck coefficient was estimated to be less than ± 1%. The thermal conductivity (λ) of the samples was calculated from the measured density, heat capacity and thermal diffusivity values. The thermal diffusivity was measured using a flash diffusivity technique [22]. The heat capacity (C) was measured on several samples using a Perkin-Elmer differential scanning calorimeter under argon atmosphere and using sapphire as the reference standard. The mass of the sample was about 60 mg, and a heating rate of 5K/min was employed. The overall error in the thermal conductivity value was estimated at about ± 10%. In light of our temperature stability results, all high temperature transport property measurements were conducted in static vacuum where the samples were found to be stable. Data for Seebeck coefficient, and electrical resistivity were recorded both upon heating and cooling.

3. RESULTS AND DISCUSSION

3.1. Physical properties

Some properties of β-Zn_4Sb_3 at room temperature are listed in Table I. The thermal-expansion coefficient is comparable to those measured for state-of-the-art thermoelectric materials Bi_2Te_3 and PbTe [23]. The measured longitudinal (v_l) and shear (v_s) sound velocities listed in Table I were used to calculate the mean sound velocity (v_m) using the following expression [24]:

$$v_m = \left(\frac{1}{3}\left[\frac{2}{v_s^3} + \frac{1}{v_l^3}\right]\right)^{-1/3} \qquad (1)$$

We calculated a mean sound velocity of 2.31 x 10^5cm s^{-1}. The Debye temperature is related to the mean sound velocity by the equation [24]:

$$\Theta = \frac{h}{k}\left[\frac{3n}{4\pi}\frac{N\,d}{M'}\right]^{1/3} v_m \qquad (2)$$

where h and k are the Planck’s and Botlzmann’s constants, respectively, N the Avogadro’s number, d the density, n the number for atoms per unit cell (n=66 for the hexagonal cell) and M’ the molecular weight of the solid. We calculated a Debye temperature of 237K for β-Zn_4Sb_3. The Debye temperature for Bi_2Te_3 and PbTe is 165 and 160K, respectively [25]. A Grüneisen constant of 1.57 was calculated using the formalism developed by Slack [26].

The results of the TGA measurements are shown in Fig . 1 where the weight loss of a sample of β-Zn_4Sb_3 is shown as a function of time and temperature in argon atmosphere. The data show that even at the highest temperature, 673K, the sample did not loose any weight. Similar tests conducted in static vacuum also showed that the samples were stable up to the same temperature. The samples used for TGA experiments were subsequently analyzed by microprobe analysis and were found to be consisting of one single phase: β-Zn_4Sb_3. The stability of the samples was also tested by annealing samples of β-Zn_4Sb_3 in sealed quartz ampoules under argon or vacuum at 673K for about 5 days. In both cases, no significant changes in the electrical resistivity were found before and, after the anneals, microprobe analysis of the samples showed that no dissociation occurred. In order to further test the stability of β-Zn_4Sb_3, the electrical resistivity of several hot-pressed samples was measured as a function of time and at different temperatures in dynamic vacuum using the van der Pauw method. The results are shown in Fig. 2 and show that no significant variation of the electrical resistivity of the sample was observed up to a temperature of 543K. For prolonged exposures of the samples at higher temperatures, the electrical resistivity of the samples increased and inclusions of ZnSb were found in the sample by microprobe analysis, likely due to some Sb losses. Additionally, the stability of β-Zn_4Sb_3 was tested in static vacuum by conducting successive Seebeck coefficient, electrical resistivity and thermal conductivity measurements on a same sample and under the same measurement conditions. The results, presented in the following section, show that the data obtained reproduce after cycling through the measurement history, demonstrating the stability of the samples up to 673K.

3.2. Transport properties

A total of about 20 samples were hot-pressed and their properties measured. All samples had high carrier concentration and p-type conductivity with similar thermoelectric properties and little variation in carrier concentration. Typical room temperature properties of hot-pressed β-Zn_4Sb_3 are listed in Table II and are characteristic of a heavily doped semiconductor. The Hall mobility values are relatively large at this doping level but relatively low compared to values on the order of 1000 $cm^2\ V^{-1}\ s^{-1}$ reported by Ugai et al. [17] at a doping level of 8.8 x 10^{17} cm^{-3}. However, these large values are in contradiction with some results obtained later by the same authors [18]. The relative complexity of the Zn-Sb phase diagram makes the preparation of single phase samples difficult and might explain the discrepancies in the results. Unfortunately, no details were given by Ugai et al. [17] on the compositional analyses of their samples.

The typical temperature dependence of the Seebeck coefficient and electrical resistivity for hot-pressed β-Zn_4Sb_3 samples are shown in Fig. 3 and Fig. 4, respectively. The Seebeck coefficient and electrical resistivity increase up to about 623K where an onset of mixed conduction seems to appear, lowering the electrical resistivity and Seebeck coefficient. Measurements were limited to 673K because of the transformation of Zn_4Sb_3 from the β to γ phase at higher temperatures and it is difficult to establish the intrinsic behavior because of the small temperature range where it seems to occur. The results of the Seebeck coefficient measurements are in agreement with the results of Tapiero et al. [15]. A maximum power factor (α^2/ρ) of 12.8 μWcm^{-1}K^{-2} was calculated at 670K. The room temperature Seebeck coefficient values are relatively large for this doping level. We estimated the hole effective mass using a single parabolic band model with acoustic phonon scattering. In this model, the Seebeck coefficient can be expressed as [27]:

$$\alpha = \pm \frac{k}{e}\left\{2\frac{F_1(\xi)}{F_0(\xi)} - \xi\right\} \qquad (3)$$

where ξ is the reduced Fermi level and F_x is a Fermi integral of order x. Using the same formalism, the carrier concentration can be expressed as:

$$p = \frac{4}{\sqrt{\pi}}\left(\frac{2\pi m^* kT}{h^2}\right)^{3/2} F_{1/2}(\xi) \qquad (4)$$

where m* is the effective mass and T is the temperature in K. The Fermi level can be calculated from the experimental Seebeck coefficient value using equation (3) and used, together with the experimental Hall carrier concentration value to calculate the effective masses from equation (4). Using the data listed in Table II, we calculated a hole effective mass of $1.18m_0$ for β-Zn_4Sb_3 (m_0 is the free electron mass). This is a fairly large effective mass and explains why the Seebeck coefficient values are relatively large.

The results of the heat capacity measurements are shown in Fig. 5. The heat capacity increases slightly from room temperature up to about 650K. Finally, Fig. 6 shows the thermal conductivity values of β-Zn_4Sb_3 between room temperature and about 650K. In this temperature range, the values are much lower than those for the state-of-the-art p-type thermoelectric materials PbTe- and Bi_2Te_3-based alloys as well as for TAGS (Te-Ag-Ge-Sb alloys). The room temperature value is about 9 mWcm^{-1}K^{-1} and decreases to about 7 mWcm^{-1}K^{-1} at 650K. A low thermal conductivity is one of the most interesting feature of β-Zn_4Sb_3. This is the lowest of all the thermoelectric materials known until now. The thermal conductivity is the sum of an electronic contribution (λ_e) and a lattice thermal conductivity (λ_L). Because our samples have relatively high hole densities, the electronic contribution can be substantial. This contribution (λ_e) can be calculated using the Wiedemann-Franz law:

$$\lambda_e = LT/\rho \qquad (5)$$

where L is the Lorenz number. Similarly to the Hall coefficient and Seebeck coefficient, the Lorenz number can be expressed as [27]:

$$L = \frac{k^2}{e^2} \frac{3\,F_0(\xi)\,F_2(\xi) - 4\,F_1^2(\xi)}{F_0^2(\xi)} \qquad (6)$$

The reduced Fermi level value, obtained from the experimental Seebeck coefficient value using equation (3), was used to calculate the Lorenz number. λ_e was then calculated as a function of temperature using the calculated Lorenz numbers and the experimental resistivity data. The results are shown in Fig. 6. The calculated room temperature lattice thermal conductivity is about 6.5 mW cm^{-1} K^{-1}. The phonon mean free path (ℓ) can be calculated from the Debye formula:

$$\lambda = C v_m \ell / 3 \qquad (7)$$

Using the typical room temperature values of $\lambda =$ 9 mW cm^{-1} K^{-1}, $v_m = 2.31 \times 10^5$ cm s^{-1}, and C= 0.22 J g^{-1} K^{-1}, we calculated a phonon mean free path of about 4.2 Å which is lower than the lattice parameter. As pointed out by Ioffe [28], this indicates that the transmission of heat may be described on the basis of lattice vibrations as "hopping" from one atom to another as opposed to Umklapp processes.

The lattice thermal conductivity can be estimated as follows [6]. The theoretical lattice thermal conductivity $\lambda'(\Theta)$ at the Debye temperature is given by:

, (8)

where $\overline{M}$ is the average mass of an atom of the crystal, δ^3 is the average volume occupied by an atom, Θ is the Debye temperature, n is the number of atoms per unit cell, γ is the Grüneisen constant at T = Θ, and B = 3.17×10^7 s^{-3} K^{-3}. For β-Zn_4Sb_3, M = 89.3 g, Θ = 237K, and n =66 for the hexagonal cell. The theoretical lattice thermal conductivity obtained from equation (8) for β-Zn_4Sb_3 is 11.45 mW cm^{-1} K^{-1} at room temperature. This is in relatively good agreement with the experimental room temperature lattice thermal conductivity of 6.5 mW cm^{-1} K^{-1} considering that the formalism used in equation (8) does not capture some phonon scattering mechanisms such as charge carrier-phonon scattering and disorder which might further reduce the lattice thermal conductivity. The thermal conductivity values for β-Zn_4Sb_3 are typical of glass-like materials. This is presumably due to its complex crystal structure and also to the presence of some antistructure defects resulting in a highly disordered structure. However, glass-like materials such as Tl_3AsSe_3 have usually high electrical resistivity [29] which is not desirable to achieve high figures of merit. This is not the case for β-Zn_4Sb_3. In this compound, there is a unique combination of low thermal conductivity and good electrical resistivity which make it a very interesting thermoelectric material.

The dimensionless thermoelectric figure of merit ZT is a function of the electrical resistivity, the Seebeck coefficient and the thermal conductivity ($ZT = \alpha^2/\rho\lambda$). The calculated figure of merit values for typical p-type β-Zn_4Sb_3 samples are shown in Fig. 7. This figure reveals that there is a gap between the low temperature state-of-the-art thermoelectric materials (Bi_2Te_3-based alloys) and the intermediate temperature materials (PbTe-based alloys) and TAGS (Te-Ag-Ge-Sb). High ZT values have been recently obtained on p-type Ce and La-based filled skutterudite compositions with a maximum ZT value of 1.4 at 850K (see Fig. 7) [11,12]. However, p-type β-Zn_4Sb_3 has the highest thermoelectric figure of merit in the 500 to 650K temperature range with a maximum value of 1.3 at about 670K. β-Zn_4Sb_3 fills in the existing gap in ZT in this temperature range. Although TAGS-based compositions have also a good thermoelectric figure of merit in this temperature range, they have been little used due to their high sublimation rate and low temperature phase transition [30]. Further studies should aim at investigating the doping of this compound to produce n-type samples and also optimize the doping level. Because of the very low room temperature thermal conductivity, it might be possible to optimize this material for thermoelectric cooling applications. Initial studies of the properties of $Zn_{4-x}Cd_xSb_3$ solid solutions have also shown that higher figures of merit might be achievable because of the decrease of the thermal conductivity due to an increase in phonon scattering rates due to point defects [31]. For many applications using thermoelectric generators, the cost of the material is important. β-Zn_4Sb_3 is relatively inexpensive compared to state-of-the-art thermoelectric materials and is an excellent candidate for thermoelectric applications, particularly for power generation.

There are several potential applications for relatively efficient thermoelectric power generators in this temperature range. Thermoelectric generators operating on natural gas, propane or diesel were built and used Bi_2Te_3 or PbTe alloys depending on the maximum hot side temperature (up to 873K) [32]. Despite their relatively low efficiency, these devices are used in various industrial applications because of their high reliability, low maintenance and long life, in particular when considering harsh environments. The most common applications are for cathodic protection, data acquisition and telecommunications. More recently, there has been a growing interest for waste heat recovery power generation, using various heat sources such as the combustion of solid waste, geothermal energy, power plants, and other industrial heat-generating processes [33-35]. There is currently an important effort in Japan to develop large scale waste heat recovery thermoelectric generators using state-of-the-art materials. For such systems, one of the most important factor is cost, and β-Zn_4Sb_3 -based materials should be less expensive (and more environmentally friendly) than current materials. But perhaps the automobile industry is the market with the most potential. Because of the need for cleaner, more efficient cars, car manufacturers worldwide are interested in using the waste heat generated by the vehicle exhaust to replace or supplement the alternator [36-38]. According to some car manufacturers, the available temperature range would be from 350 to 800K, which is matched perfectly by the performance of β-Zn_4Sb_3 -based materials.

5. SUMMARY

Thermoelectric properties of β-Zn_4Sb_3 were measured on hot-pressed samples. Exceptionally low thermal conductivity was measured and a maximum ZT value of 1.3 was achieved at 670K. The good thermoelectric performance of p-type β-Zn_4Sb_3 fills the gap in ZT values between the low temperature state-of-the-art thermoelectric materials Bi_2Te_3-based alloys and the intermediate temperature materials PbTe-based alloys and TAGS (Te-Ag-Ge-Sb). The stability of the material was studied and it was found that the thermoelectric properties remain stable up to 670K under static vacuum and argon. This material, relatively inexpensive, could be used in thermoelectric power generators and a brief description of the numerous potential applications was given. Efforts should now focus on producing n-type samples and studying the alloying of this compound with other isostructural compounds such as Cd_4Sb_3 which already has been identified as a promising route to achieve even higher ZT values.

ACKNOWLEDGMENTS

The work described in this paper was carried out at the Jet Propulsion Laboratory/California Institute of Technology, under contract with the National Aeronautics and Space Administration. The authors would like to thank Danny Zoltan and Andy Zoltan for thermoelectric property measurements.

REFERENCES

1. Caillat T., Borshchevsky A., and Fleurial J. -P., in *Proceedings of the XIth International Conference on Thermoelectrics*, University of Texas at Arlington, edited by K. R. Rao (University of Texas at Arlington Press, Arlington), p. 98 (1993).
2. Slack G. A. and Tsoukala V.G., *J. Appl. Phys.* **76** 1665 (1994).
3. Morelli D.T., Caillat T., Fleurial J. -P., Borshchevsky A., Vandersande J., Chen B., and Uher C., *Phys. Rev.* **B52** 4926 (1995).
4. Sharp J.W., Jones E.C., Williams R.K., Martin P.M., Sales B.C., *J. Appl. Phys.* **78** 1013 (1995)
5. Mandrus D., Migliori A., Darling T. W., Hundley M. F., Peterson E. J., Thompson J. D., *Phys. Rev*. **B 52** 4926 (1995).
6. Caillat T., Fleurial J. -P., Borshchevsky A., *J. Appl. Phys.* **79** (11) 8419 (1996).
7. Caillat T., Fleurial J. -P., Borshchevsky A., *J. Appl. Phys.* **80** (8) 4442 (1996).

8. Caillat T., Fleurial J. -P., Borshchevsky A., *J. Crystal Growth*, **166** 722 (1966).

9. Morelli D. T. and Meisner G. P., *J. Appl. Phys***.** **77** 3777 (1995).

10. Nolas G. S., Slack G. A., Tritt T. M., Morelli D. T., *Proceedings of XIVth International Conference on Thermoelectrics*, St. Petersburg, Russia, edited by M. V. Vedernikov, A. F. Ioffe Physical-Technical Institute, 194201, St-Petersburg, Russia, p. 236 (1995).

11. Fleurial J. -P., Borshchevsky A., Caillat T., Morelli D.T., Meisner G. P., *Proceedings of the XV International Conference on Thermoelectrics,* Pasadena, CA, USA, IEEE Catalog Number 96TH8169, pp. 91-95 (1996).

12. Sales B. C., Mandrus D., Williams R. K., *Science* **272** 1352 (1996).

13. Mayer H. W., Mikhail I., and Schubert K., *J. Less Common Metals* **59**, 43 (1978).

14. Tydlitat V., *Czech. J. Phys*. **9**, 638 (1959).

15. Tapiero M ., Tarabichi S., Gies J. G., Noguet C., Zielinger J. P., Joucla M., Loison J., Robino M., and Henrion J., *Solar Energy Materials* **12**, p. 257 (1985).

16. Spitzer D., *J. Phys. Chem. Solids* **31**, 19 (1970).

17. Ugai Ya. A., Averbakh E. M., and Lavrov V. V., *Sov. Phys. Solid State* **4**, 2393 (1963).

18. Ugai Ya. A., Marshakova T. A., Shevchenko V. Ya., and Demina N. P., *Inorg. Mat.* **5**, 1180 (1969).

19. Psarev V. I. and Kostur N. L., *Izv. Vyssh. Ucheb. Zaved. Fiz.* **10**, (2), 34 (1967).

20. McCormack J. and Fleurial J. -P., *Modern Perspectives on Thermoelectric and Related Materials* (Edited by D. D. Alred, C. B. Vining and G. A. Slack), Materials Research Society, Pittsburgh, p. 135 (1991).

21. Wood C., Zoltan D., and Stapfer G., *Rev. Sci. Instrum.* **56**, 179 (1985).

22. Vandersande J. W., Wood C., Zoltan A., and Whittenberger D., *Thermal Conductivity*, Plenum Press, New York, p. 445 (1988).

23. Fano V., *CRC Handbook of Thermoelectrics* (Edited by D.M. Rowe), p. 257, Boca Raton, New York (1995).

24. Anderson O. L., *J. Phys. Chem. Solids* **24**, 909 (1963).

25. Slack G. A., *CRC Handbook of Thermoelectrics* (Edited by D.M. Rowe), CRC Press, Boca Raton, New York, p. 407, (1995).

26. Slack G. A., Solid State Physics, editors H. Ehrenreich, F. Steiz, and D. Turnbull (Academic, New York) vol 34, p.1 (1979).

27. V. I. Fistul, *Heavily Doped Semiconductors* (Plenum Press, New York), (1969).

28. Ioffe A. F., *Sov. Phys. Solid State* **1**, 141 (1959).

29. Ewbank M. D., Newman P. R., and Kuwamoto H., *J. Appl. Phys.* **53**, (9), 6450 (1982).

30. Skrabeck E. and Trimmer D. S., *CRC Handbook of Thermoelectrics* (Edited by D.M. Rowe), CRC Press, Boca Raton, New York, p. 267 (1995).

31. Caillat T., Borshchevsky A., and Fleurial J. -P., in *Proceedings of the 31st Intersociety Energy Conversion Engineering Conference*, Washington, DC, August 11-16, p. 905 (1996).
32. Naughton A. G., *CRC Handbook of Thermoelectrics* (Edited by D.M. Rowe), CRC Press, Boca Raton, New York, p. 459 (1995).
33. Rowe D. M., Matsuura K., Koumoto K., Tsumura H., and Tsuyoshi A., in *Proceedings of the XII Int. Conf. on Thermoelectrics*, edited by K. Matsuura, Yokohama, Japan, November 9-11, p.463 (1993).
34. Matsuura K., in *Proceedings of the XII Int. Conf. on Thermoelectrics*, edited by K. Matsuura, Yokohama, Japan, November 9-11, p. 439 (1993).
35. Kajikawa T., Ito M., Shibuya E., and Hirayama N., in *Proceedings of the XII Int. Conf. on Thermoelectrics*, edited by K. Matsuura, Yokohama, Japan, November 9-11, p. 491 (1993).
36. Takanose E. and Tamakoshi H., in *Proceedings of the XII Int. Conf. on Thermoelectrics*, edited by K. Matsuura, Yokohama, Japan, November 9-11, p. 467 (1993).
37. Morelli D. T., to be published in the *Proceedings of the XV International Conference on Thermoelectrics*, Pasadena, CA, March 26-29 (1996).
38. Bass J. C., Elsner N. B., and Leavitt F. A, in *Proceedings of the XIII Int. Conf. on Thermoelectrics*, Kansas City, MO, p. 295 (1994).

Table I

Property	Units	β-Zn_4Sb_3
Melting point	K	836 [13,17]
Lattice parameters	Å	a=12.231 c=12.428 [13]
Energy bandgap	eV	1.2 [14,15]
X-ray density	g/cm^3	6.077
Thermal expansion coefficient	1/K	1.93×10^{-5}
Shear sound velocity	10^5 cm/s	3.59
Transversal sound velocity	10^5 cm/s	2.08
Grüneisen constant	....	1.57
Debye temperature	K	237

Table II

Property	Units	β-Zn_4Sb_3
Conductivity type	......	p
Electrical resistivity	mΩ.cm	2
Hall mobility	$cm^2\ V^{-1}\ s^{-1}$	30
Hall carrier concentration	$10^{19}\ cm^{-3}$	9
Seebeck coefficient	$\mu V\ K^{-1}$	113
Thermal conductivity	$mW\ cm^{-1}\ K^{-1}$	9

Tables Captions

Table I: Some physical parameters of β-Zn_4Sb_3 at room temperature

Table II: Typical room temperature thermoelectric properties of β-Zn_4Sb_3 hot-pressed samples

Figures Captions

Figure 1: Weight loss as a function of time and temperature for a β-Zn_4Sb_3 hot-pressed sample under Argon atmosphere and using a heating rate of 5K/min. No weight loss is observed up to 650K indicating the stability of the compound in this environment up to this temperature.

Figure 2: Electrical resistivity as a function of time and temperature for a β-Zn_4Sb_3 hot-pressed sample in dynamic vacuum (the dashed lines correspond to the electrical resistivity and temperature variations for the sample maintained at a temperature of 543K and the plain lines up at 513K). The results indicate the stability of the compound up to about 513K in this environment.

Figure 3: Typical variations of the Seebeck coefficient as a function of temperature for β-Zn_4Sb_3 hot-pressed samples. The data shown are for a sample subjected to the following measurement cycle: (a) Seebeck coefficient-1 (b) electrical resistivity-1 (c) thermal conductivity-1 (d) Seebeck coefficient-2 (e) electrical resistivity-2 (f) thermal conductivity-2

Figure 4: Typical variations of the electrical resistivity as a function of inverse temperature for β-Zn_4Sb_3 hot-pressed samples. The data shown are for a sample subjected to the following measurement cycle: (a) Seebeck coefficient-1 (b) electrical resistivity-1 (c) thermal conductivity-1 (d) Seebeck coefficient-2 (e) electrical resistivity-2 (f) thermal conductivity-2

Figure 5: Typical variations of the heat capacity as a function of temperature for β-Zn_4Sb_3 hot-pressed samples.

Figure 6: Typical variations of the thermal conductivity as a function of temperature for β-Zn_4Sb_3 hot-pressed samples and state-of-the-art thermoelectric materials.

The dashed line represents the calculated lattice thermal conductivity for β-Zn_4Sb_3. The data shown are for a sample subjected to the following measurement cycle: (a) Seebeck coefficient-1 (b) electrical resistivity-1 (c) thermal conductivity-1 (d) Seebeck coefficient-2 (e) electrical resistivity-2 (f) thermal conductivity-2

Figure 7: Typical variations of the thermoelectric figure of merit ZT as a function of temperature for β-Zn_4Sb_3 hot-pressed samples and state-of-the-art thermoelectric materials.

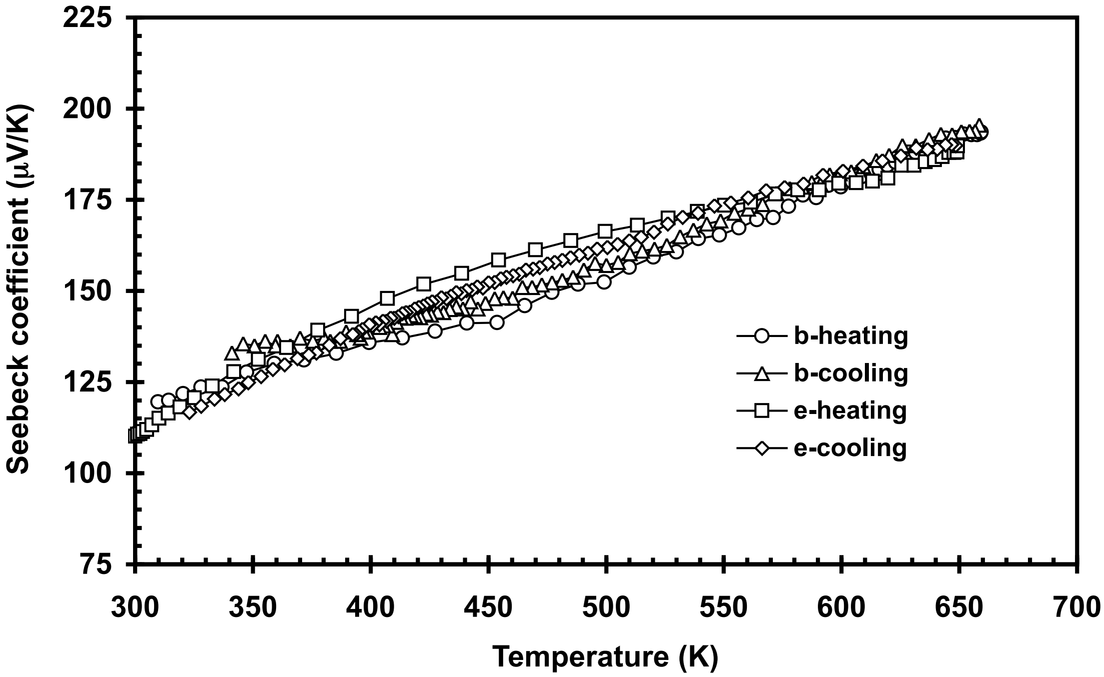

225
200
175
150
125
100
75
Seebeck coefficient (μV/K)
300
350
400
450
500
550
600
650
700
Temperature (K)
b-heating
b-cooling
e-heating
e-cooling

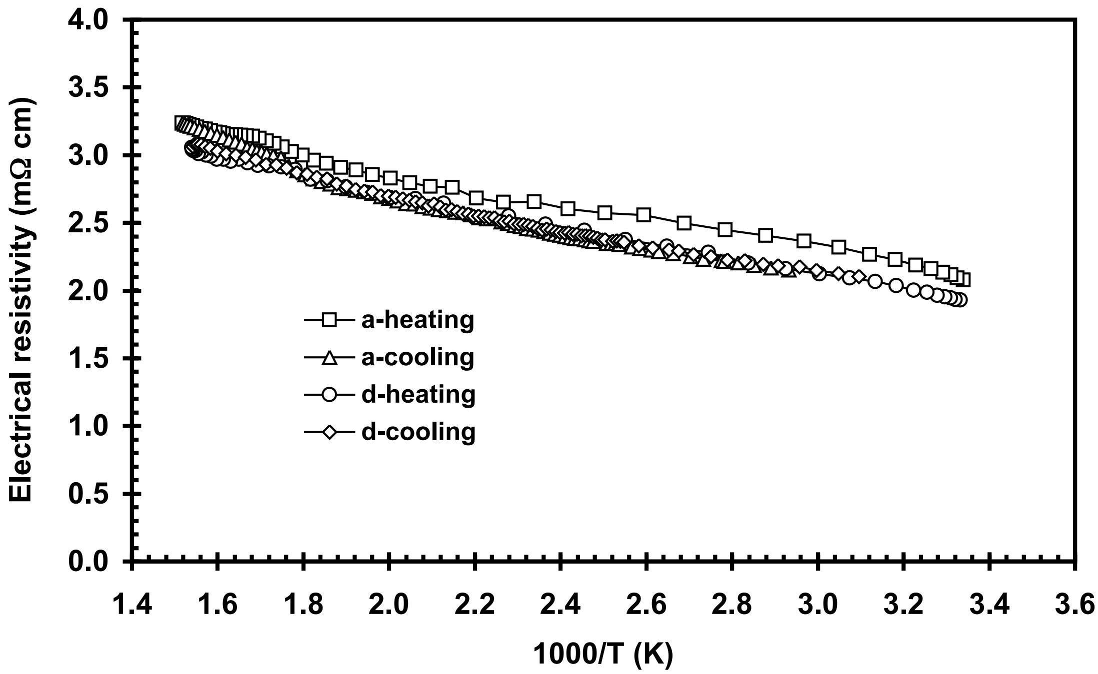

4.0
3.5
3.0
2.5
2.0
1.5
1.0
0.5
0.0
Electrical resistivity (mΩ cm)
1.4
1.6
1.8
2.0
2.2
2.4
2.6
2.8
3.0
3.2
3.4
3.6
1000/T (K)
a-heating
a-cooling
d-heating
d-cooling

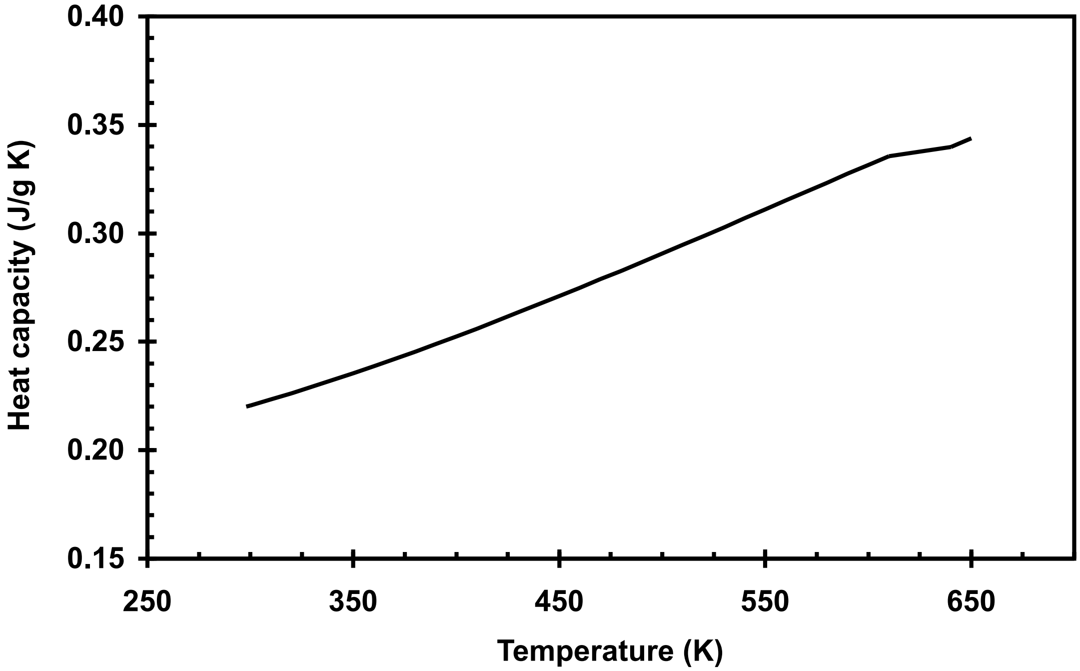

Heat capacity (J/g K)
0.40
0.35
0.30
0.25
0.20
0.15
250
350
450
550
650
Temperature (K)

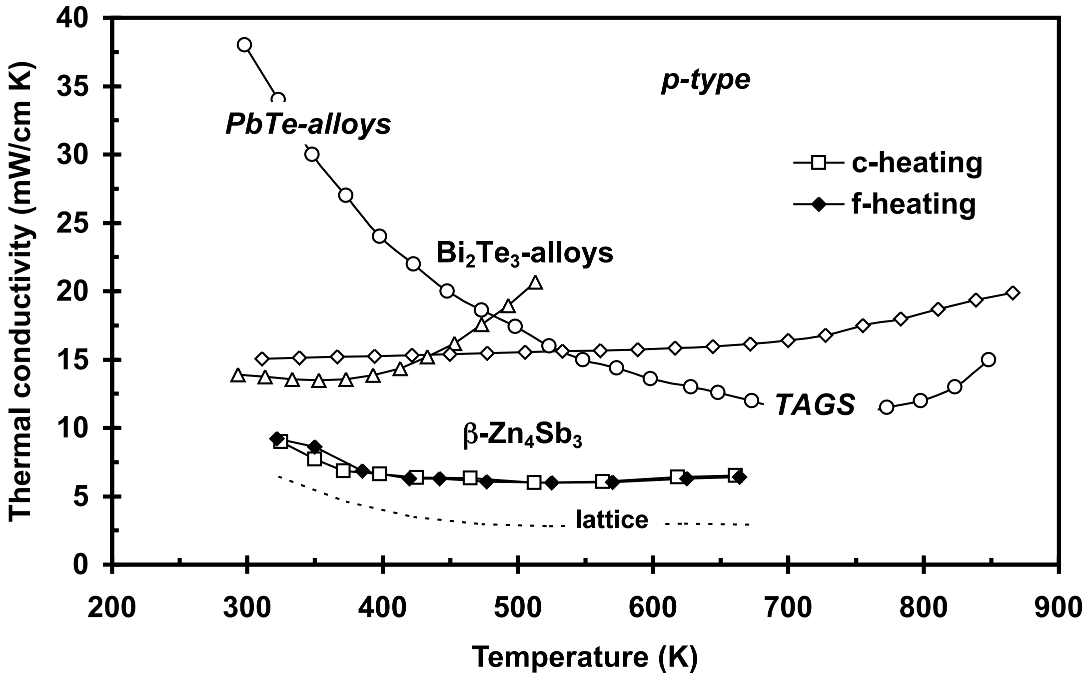
p-type
PbTe-alloys
c-heating
f-heating
Bi2Te3-alloys
TAGS
β-Zn4Sb3
lattice
Thermal conductivity (mW/cm K)
Temperature (K)
0
5
10
15
20
25
30
35
40
200
300
400
500
600
700
800
900